Coupling between the N- and C-Terminal Domains Influences Transducin-α Intrinsic GDP/GTP Exchange†

Khakim G. Muradov and Nikolai O. Artemyev*

Department of Physiology and Biophysics, University of Iowa College of Medicine, Iowa City, Iowa 52242

Received September 17, 1999; Revised Manuscript Received February 1, 2000

ABSTRACT: The N-terminal regions of the heterotrimeric G-protein α-subunits represent one of the major G$\beta\gamma$ contact sites and have been implicated in an interaction with G-protein-coupled receptors. To probe the role of the N-terminal domain of transducin-α in G-protein function, a chimeric Gtiα subunit with the 31 N-terminal Gtα residues replaced by the corresponding 42 residues of Gsα (Ns-Gtiα) has been examined for the interaction with light-activated rhodopsin (R*). Gtiα displayed a somewhat higher R*-stimulated rate of GTPγS binding relative to Ns-Gtiα, suggesting modest involvement of the Gtα N-terminal sequence in recognition of the receptor. However, the intrinsic rate of nucleotide exchange in Ns-Gtiα was significantly faster (k_{app} = 0.014 min^{-1}) than that in Gtiα (k_{app} = 0.0013 min^{-1}) as judged by the GTPγS binding rates. Substitution of 42 N-terminal residues of Gsα by the Gtα residues in a reciprocal chimera, Nt-Gsα, had an opposite effect—notable reduction in the intrinsic GTPγS-binding rate (k_{app} = 0.0075 min^{-1}) in comparison with Gsα (k_{app} = 0.028 min^{-1}). Residue Val30 (His41 in Gsα) within the N-terminal region of Gtα interacts with the C-terminal residue, Ile339. To test the hypothesis that observed changes in the intrinsic nucleotide exchange rate in chimeric Gα subunits might be attributed to this interaction, GtiαVal30His, GtiαIle339Ala, and Ns-GtiαHis41Val mutants have been made and analyzed for basal GTPγS binding. GtiαVal30His and GtiαIle339Ala had increased GTPγS binding rates (k_{app} = 0.010 and 0.009 min^{-1}, respectively), whereas Ns-GtiαHis41Val had a decreased GTPγS binding rate (k_{app} = 0.0011 min^{-1}) relative to their parent proteins. These results suggest that the coupling between the N-terminal and C-terminal domains of Gtα is important for maintaining a low nucleotide exchange rate in unstimulated transducin.

The visual transduction cascade in vertebrates is a classical G-protein signaling pathway with a characteristic low noise and high gain signal amplification. In the dark, the rate of basal GDP−GTP exchange on photoreceptor G-protein transducin (Gtα$\beta\gamma$)[1] is very slow (10^{-6} s^{-1}). Photoexcited rhodopsin (R*) accelerates the exchange rate up to 10^3 s^{-1}. The key rate-limiting step catalyzed by R* is GDP release. GTP binding to the empty nucleotide pocket on Gtα is driven by conformational changes that it causes followed by dissociation of Gtα from Gt$\beta\gamma$ and R* (*1, 2*). Extensive biochemical studies coupled with the solution of crystal structures of transducin have provided a basis for modeling the mechanisms of R*-induced Gt activation (*3*−*6*). The lipid modifications, heterogeneous acylation at the Gtα N-terminus and farnesylation of the Gγ C-terminus, suggest a presumable orientation of the transducin molecule on the photoreceptor disk membrane (*5*). The main R* interaction sites, the C-terminus (Gtα-340−350) and α4-β6 loop (aa 305−315), are localized on the receptor surface of Gtα that faces the membrane. The key receptor recognition determinant is the Gtα C-terminus. An original finding that ADP-ribosylation of Gtα Cys347 by pertussis toxin uncouples Gt from R* (*7, 8*) has been supported and extended by mutational and synthetic peptide analyses (*9*−*11*). Binding of R* to Gtα-340−350 and the Gtα α4-β6 loop at the membrane surface is likely to trigger conformational changes of Gtα that are transmitted via the α5 helix and the β6 sheet to the β6-α5 loop. The Gtα β6-α5 loop contains the guanine ring binding residues, and GDP release occurs when these residues are "disturbed" by receptor binding (*5, 6*). Gt$\beta\gamma$ is absolutely required for effective activation of Gt. Direct interaction of R* with Gt$\beta\gamma$ (*12, 13*) may participate in Gt activation by conformationally altering the switch I/switch II region via Gtβ/Gtα contacts and facilitating release of GDP (*6*).

The role of the N-terminal region of Gtα in the interaction with R* is not fully understood. The N-terminus constitutes one of the two Gtα/Gt$\beta\gamma$ interaction interfaces. The N-terminal acylation (myristoylation) contributes to the membrane attachment and stability of the Gtα$\beta\gamma$ complex on the membrane, which is essential for Gt activation (*14*). Also, in all probability, the lipid insertion into the membrane brings the N-terminus close to intracellular loops of R*. However, it is not clear whether the N-terminal domain directly interacts with R*. A synthetic peptide corresponding to Gtα-8−23 competed with Gtα for binding to R* in the MII

†This work was supported by National Institutes of Health Grant 2RO1 EY-10843. NIH Grant DK-25295 supported the services provided by the Diabetes and Endocrinology Research Center of the University of Iowa.

* Correspondence should be addressed to this author. Tel.: 319/335-7864, FAX: 319/335-7330, E-mail: nikolai-artemyev@uiowa.edu.

[1] Abbreviations: Gtα, rod G-protein (transducin) α-subunit; Gt$\beta\gamma$, transducin $\beta\gamma$ subunits; R*, light-activated (bleached) rhodopsin; ROS, rod outer segment(s); uROS, urea-stripped ROS membranes; GTPγS, guanosine 5′-O-(3-thiotriphosphate).

10.1021/bi992156l CCC: $19.00
Published on Web 03/16/2000

stabilization assays. But unlike Gtα-340−350, Gtα-8−23 was unable to mimic Gtα$\beta\gamma$ effects on MII formation (*11*). Ala-scanning mutational analysis of Gtα revealed defects of R* activation only in those Gtα N-terminal mutants that had substitutions of the Gtβ contact residues (*15*). In addition to a potential role in the interaction with R*, the N-terminal domain of Gtα may be involved in maintaining a low basal GDP/GTP exchange rate on Gtα. Loss of interactions between the N- and C-terminal regions was thought to lead to decreased affinity of truncated Goα and Giα for GDP (*16, 17*).

In this study, we examined roles of the N-terminal region in intrinsic GDP/GTP exchange and in Gtα activation by R* using chimeric Gsα/Gtiα proteins containing the N-terminal domains of Gtα or Gsα. Chimeras between Gtiα and Gsα were designed because Gsα showed no appreciable interaction with the visual receptor.

EXPERIMENTAL SECTION

Materials. [^{35}S]GTPγS (1160 Ci/mmol) was purchased from Amersham Pharmacia Biotech. Restriction enzymes were from New England Biolabs. T4 DNA ligase was from Boehringer Mannheim. Cloned Pfu DNA polymerase was from Stratagene. TPCK-treated trypsin was from Worthington Biochemical Corp. All other chemicals were from Sigma or Fisher. Bovine ROS membranes were prepared as previously described (*18*). Urea-washed ROS membranes (uROS) were prepared according to the protocol in Yamanaka et al. (*19*). Gt$\beta\gamma$ was purified according to Kleuss et al. (*20*).

Cloning and Site-Directed Mutagenesis of Chimeric Gtiα and Gsα. Chimeric Gtiα subunit, Ns-Gtiα, with the 31 N-terminal Gtα residues replaced by the corresponding 42 residues of Gsα was made using the pHis6-Gsα vector for expression of Gsα (*21*) as a template in the first round of PCR amplification. The PCR reaction included a forward primer carrying a *Nco*I site with a start codon for Gsα cDNA and a reverse primer coding for the sequence Gsα-37−42 linked to Gtα-32−39. The PCR product was then used as a forward primer in a second round of PCR amplification with the vector for expression of Gtα/Giα$_1$ chimera 8 (pHis6-Gtiα) as a template (*22*). A reverse primer contained a *Bam*HI site overlapping codons for residues Gtα-207−209. The PCR product was digested with *Nco*I and *Bam*HI and subcloned into pHis6-Gtiα. Chimeric Gsα's with 42 N-terminal residues of Gsα substituted by the 31 N-terminal Gtα residues, Nt-Gsα and Nt-Gsα-Ct, were generated using the pHis6-Gtiα vector as a template in the first PCR round. A forward primer carried a *Nco*I site with a start codon for Gtiα cDNA and a reverse primer coding for the sequence Gtα-25−31 linked to Gsα-43−49. The PCR product was paired with a reverse primer containing a *Hin*dIII site and a stop codon of Gsα in a second round of PCR amplification with pHis6-Gsα as a template. The PCR product was then cut with *Nco*I and *Bgl*II (a *Bgl*II site overlaps codons for residues Gsα-294−296) and ligated to the large *Nco*I/*Bgl*II fragments of pHis6-Gsα and pHis6-Gsα-Ct (*23*). Similar two-round PCR procedures were utilized to make mutant proteins. Gtiα mutants, Val30Ala and Val30His, were obtained using pHis6-Gtiα as a template, a forward primer with a *Nco*I site, and reverse primers coding for these mutations in the first PCR round. The PCR products were used as forward primers in the second PCR round on the same template with the reverse primer containing a *Bam*HI site. Mutants Ns-GtiαHis41Val and GsαHis41Val were generated using an analogous two-step PCR mutagenesis with pHis6-Ns-Gtiα and pHis6-Gsα as templates, respectively. The Gtiα mutations Ile339Ala and Ile339His were introduced using a one-step PCR procedure with a forward primer containing a *Bam*HI site and reverse primers carrying mutations, a *Hin*dIII site, and a stop codon. Sequences of all chimeras and mutants were confirmed by automated DNA sequencing at the University of Iowa DNA Core Facility.

Typically, for protein expression, 500 mL of 2×TY media was inoculated with 10 mL of overnight culture of BL21-(DE3) cells transformed with chimeric or mutant Gα DNAs. At A_{600} = 0.8, expression was induced by 30 μM IPTG for 3 h at 24 °C. Cells were pelleted and kept frozen at −70 °C. Purifications of recombinant proteins were carried out as described (*22, 24*). Yields for 80−90% pure Gα's were normally 3−5 mg.

Trypsin Protection Assay. Mutant Gα's (20 μM) were incubated for 5 min at 25 °C in 20 mM HEPES buffer (pH 8.0) containing 130 mM NaCl, 50 μM GDP, and 5 mM $MgSO_4$. Where indicated, 10 mM NaF and 30 μM $AlCl_3$ were included in the buffer. Trypsin digestions were performed with 25 μg of trypsin/mL for 15 min at 25 °C and stopped with simultaneous addition of SDS sample buffer and heat treatment (100 °C, 5 min).

GTPγS Binding Assay. Gα's (1 μM) alone or mixed with 2 μM Gt$\beta\gamma$ or 2 μM Gt$\beta\gamma$ and uROS membranes (100 nM rhodopsin for Gtiα and its mutants; 300 nM for Gsα and its mutants) in 20 mM Tris-HCl (pH 8.0) buffer containing 130 mM NaCl, 10 mM $MgSO_4$, and 10 mM dithiothreitol (buffer A) were incubated for 3 min at 25 °C. Binding reactions were started by addition of 5 μM [^{35}S]GTPγS (1 Ci/mmol) in buffer A. Aliquots of 50 μL were withdrawn at the indicated times, mixed with 1 mL of ice-cold buffer A, and passed through Whatman cellulose nitrate filters (0.45 μm). The filters were then washed 2 times with buffer A (2 mL, ice-cold). Upon complete dissolution in a 3a70B cocktail, the filters were counted in a liquid scintillation counter. The k_{app} values for the binding reactions were calculated by fitting the data to the equation: GTPγS bound (% bound) = $100 \times (1 - e^{-kt})$. A linear regression fit was used when less than 25% of total Gα or mutant bound GTPγS during the time course of binding reactions, and the k_{app} values were calculated as slopes of linear functions. The results are expressed as the mean ± SE of triplicate measurements.

RESULTS

Analysis of the Gtiα/Gsα Chimera Containing the Gsα N-Terminus. The N-terminal region of Gsα (42 aa) was replaced into Gtα/Giα$_1$ chimeric protein, Chi8 (*22*). Chi8 contains greater than 90% of the Gtα sequence including the Gtα N-terminal half. For clarity, Chi8 is termed Gtiα throughout the text. Gtiα is fully capable of interaction with Gt$\beta\gamma$ and R* (*22, 24*). As expected, Gtiα showed a low spontaneous rate of GDP release as assessed in GTPγS binding assays (k_{app} = 0.0013 min^{-1}) (Figure 1A, Table 1). The basal rate of GTPγS binding to Gtiα was practically unaffected in the presence of Gt$\beta\gamma$ (k_{app} = 0.002 min^{-1}), but the combined addition of uROS membranes (100 nM

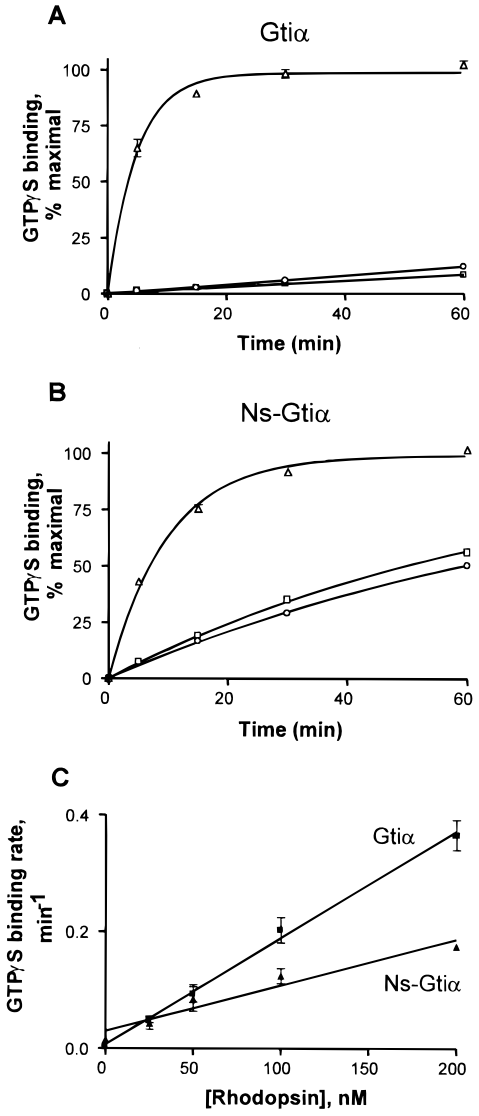

FIGURE 1: Kinetics of GTPγS binding to Gtiα and Ns-Gtiα. The binding of GTPγS to Gtiα (A) and Ns-Gtiα (B) (1 μM each) alone (□) or mixed with 2 μM Gtβγ (○) or 2 μM Gtβγ and uROS membranes (100 nM rhodopsin) (△) was initiated by addition of 5 μM [^{35}S]GTPγS. Gα-bound GTPγS was counted by withdrawing aliquots at the indicated times and passing them through Whatman cellulose nitrate filters (0.45 μm). GTPγS binding is expressed as percent of maximal, calculated based on protein concentration. The calculated k_{app} values (min^{-1}) are the following: (A) 0.0013 ± 0.0001 (□), 0.0020 ± 0.0001 (○), 0.21 ± 0.01 (△); (B) 0.014 ± 0.001 (□), 0.012 ± 0.001 (○), 0.10 ± 0.01 (△). (C) The binding of GTPγS to Gtiα (■) or Ns-Gtiα (▲) (1 μM each) was measured in the presence of 2 μM Gtβγ and ROS membranes containing the indicated concentrations of rhodopsin. The apparent GTPγS binding rates are plotted as functions of R* concentration. The apparent activation constants (10^{-6} M^{-1}·min^{-1}) calculated as slopes of the linear fits are 1.8 ± 0.1 (■) and 0.8 ± 0.1 (▲).

R*) and Gtβγ (2 μM) to Gtiα resulted in a large rate increase (k_{app} = 0.21 min^{-1}) (Figure 1A). Expression levels of soluble chimeric Gα containing the Gsα N-terminus (Ns-Gtiα) were similar to those of Gtiα (~5 mg/L of culture). The trypsin protection assay demonstrated that Ns-Gtiα was capable of undergoing an activational conformational change upon the binding of GDP·AlF_4^- (Figure 2A). In comparison to Gtiα, Ns-Gtiα demonstrated a significant (~10-fold) increase in the basal rate of GTPγS binding (k_{app} = 0.014 min^{-1}) (Figure 1B, Table 1). Importantly, this increased basal rate in Ns-Gtiα was not notably inhibited by addition of Gtβγ (k_{app} = 0.012 min^{-1}) (Figure 1B), which is known to suppress a relatively high intrinsic GDP/GTP exchange of Gsα (*25*). The lack of Gtβγ effect was not due to potential disruption of the Gα/Gβγ interaction, since together with R* Gtβγ enhanced the GTPγS binding rate of Ns-Gtiα (k_{app} = 0.10 min^{-1}) (Figure 1B). Intermediate concentrations of Gtβγ (0.25 μM) in the presence of uROS produced proportional acceleration in GTPγS binding rates of Gtiα (k_{app} = 0.036 min^{-1}) and Ns-Gtiα (k_{app} = 0.05 min^{-1}), further pointing to the intact Ns-Gtiα/Gtβγ interaction. To compare the relative abilities of Gtiα and Ns-Gtiα to interact with R*, the apparent rates of GTPγS binding to these proteins were determined at varying concentrations of ROS membranes (Figure 1C). The GTPγS binding rates were linear functions of rhodopsin concentration, and the apparent activation constants for Gtiα and Ns-Gtiα calculated as slopes in Figure 1C were 1.8 × 10^6 and 0.8 × 10^6 M^{-1} min^{-1}, respectively. The lower degree of activation of Ns-Gtiα by R* in comparison to Gtiα suggests that the N-terminal region of Gtα may contain sequence-specific determinants for receptor recognition.

Table 1: GTPγS Binding Properties of Chimeric and Mutant Gα Subunits

chimera or mutant	k_{app} values, min^{-1}		
	basal	+Gtβγ	+Gtβγ, R*
Gtiα	0.0013 ± 0.0001	0.0020 ± 0.0001	0.21 ± 0.01
Gsα	0.028 ± 0.001	0.0055 ± 0.0006	0.0075 ± 0.0005
Ns-Gtiα	0.014 ± 0.001	0.012 ± 0.001	0.10 ± 0.01
Nt-Gsα	0.0075 ± 0.0005	0.0065 ± 0.0005	0.018 ± 0.001
Gsα-Ct	0.020 ± 0.001	0.0045 ± 0.0005	0.12 ± 0.01
Nt-Gsα-Ct	0.0085 ± 0.001	0.0075 ± 0.0005	0.027 ± 0.002
GtiαVal30His	0.010 ± 0.002	0.015 ± 0.002	0.17 ± 0.01
GtiαVal30Ala	0.003 ± 0.0001	0.004 ± 0.0002	0.16 ± 0.02
GtiαIle339Ala	0.009 ± 0.0005	0.014 ± 0.001	0.33 ± 0.04
Ns-GtiαHis41 Val	0.0011 ± 0.0001	0.0014 ± 0.0001	0.11 ± 0.01
GsαHis41Val	0.012 ± 0.001	0.0015 ± 0.0002	0.002 ± 0.0002

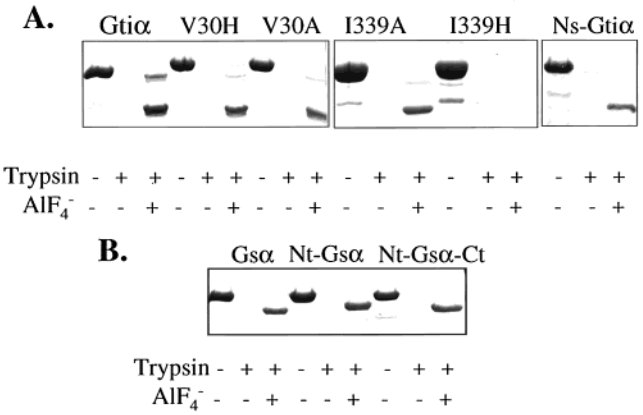

FIGURE 2: Trypsin protection test for Gtiα, mutant Gtiα, Ns-Gtiα (A) and for Gsα, Nt-Gsα, Nt-Gsα-Ct (B). SDS−polycrylamide gel (12%) stained with Coomassie Blue. Gtiα, the Val30His, Val30Ala, Ile339Ala, and Ile339His mutants of Gtiα, and Ns-Gtiα (A) or Gsα, Nt-Gsα, and Nt-Gsα-Ct (B) (20 μM each) were treated with trypsin (25 μg/mL) for 15 min at 25 °C in the absence or presence of 30 μM $AlCl_3$/10 mM NaF.

Analysis of Chimeric Gsα Containing the Gtα N-Terminus. A reciprocal to the Ns-Gtiα chimera, Nt-Gsα, has been made to further investigate the role of the Gtα N-terminus in the interaction with R*. Second, Nt-Gsα was utilized to determine if the N-terminus of Gtα can render Gsα with the low

intrinsic GDP/GTP exchange rate characteristic for transducin. The trypsin protection assay confirmed the ability of Nt-Gsα to assume an active conformation upon binding of GDP·AlF_4^- (Figure 2B). Consistent with previous reports, Gsα had a relatively high spontaneous GTPγS binding rate (k_{app} = 0.028 min^{-1}), which was sensitive to the presence of Gβγ (Table 1). Addition of a 2-fold molar excess of Gtβγ inhibited the rate of GTPγS binding to Gsα by ~5-fold (k_{app} = 0.0055 min^{-1}). As we demonstrated recently (*23*), R* and Gtβγ together only slightly stimulated the Gsα GTPγS binding rate (k_{app} = 0.0075 min^{-1}) over that in the presence of Gtβγ alone (Table 1). Substitution of 42 N-terminal residues of Gsα by the Gtα residues in Nt-Gsα had decreased the intrinsic GTPγS binding rate (k_{app} = 0.0075 min^{-1}) in comparison with Gsα, although this effect was not as strong as the opposite effect in Ns-Gtiα (Figure 3A, Table 1). Surprisingly, spontaneous GTPγS binding to Nt-Gsα was not meaningfully inhibited by Gtβγ (k_{app} = 0.0065 min^{-1}). Combined Gtβγ and R* had a moderate stimulatory effect on Nt-Gsα (k_{app} = 0.018 min^{-1}) (Figure 3A).

To test the possibility that Nt-Gsα may have impaired interaction with Gtβγ, the N-terminus of Gtα was replaced into chimeric Gsα, Gsα-Ct, containing the C-terminus of Gtα, Gtα-340−350 (Nt-Gsα-Ct). Analogously to Gsα, Gsα-Ct has a high intrinsic GDP/GTP exchange rate (k_{app} = 0.020 min^{-1}), which is suppressed by Gtβγ (0.0045 min^{-1}) (Figure 3B, Table 1). In contrast to Gsα, R* effectively enhances the nucleotide binding rate of Gsα-Ct in the presence of Gtβγ (k_{app} = 0.12 min^{-1}) (Figure 3B). Similarly to Nt-Gsα, the basal GTPγS binding rate of Nt-Gsα-Ct (k_{app} = 0.0085 min^{-1}) was insensitive to Gtβγ (k_{app} = 0.0075 min^{-1}) (Figure 3C, Table 1). R* and Gtβγ accelerated the kinetics of GTPγS binding to Nt-Gsα-Ct (k_{app} = 0.027 min^{-1}) to a lesser extent than it was seen with Gsα-Ct (Figure 3). This result suggests that chimeric Gsα's with the N-terminal domain of Gtα, Nt-Gsα and Nt-Gsα-Ct, are likely defective in their interaction with Gtβγ. Alternatively, the Nt- and Ct-terminal domains in Nt-Gsα-Ct are not optimally aligned with the corresponding binding sites in R*.

GTPγS Binding Properties of Mutant Gtiα with Substitutions of Val30 and Ile339. Crystal structures of Gtα suggest a plausible mechanism to explain the increase of intrinsic GTPγS binding rate in Ns-Gtiα. Gtα Val30 makes a contact with Ile339 at the C-end of the α5 helix. Such an interaction may increase Gtα affinity for GDP via stabilization of the α5 helix and, consequently, the β6-α5 loop. Gsα has a His residue (His41) at the corresponding position which might interfere with the N- and C-terminal coupling in Ns-Gtiα. The Gtiα Val30His, Val30Ala, Ile339His, and Ile339Ala mutants have been generated to probe the role of the interaction between Val30 and Ile339 in the control of intrinsic GDP/GTP exchange of Gtα. Gtiα Val30His, Val30Ala, and Ile339Ala were functionally expressed in *E. coli* with yields similar to Gtiα. The Ile339His mutation led to expression of inactive protein, which failed the trypsin protection test. The trypsin protection test for the Gtiα Val30His, Val30Ala, Ile339Ala, and Ile339His mutants is shown in Figure 2A. Analysis of basal GTPγS binding demonstrated that the Val30His and Ile339Ala mutants had significantly increased GTPγS binding rates (k_{app} values of 0.010 and 0.009 min^{-1}, respectively) in comparison with Gtiα (Figure 4, Table 1). The GtiαVal30Ala mutation had

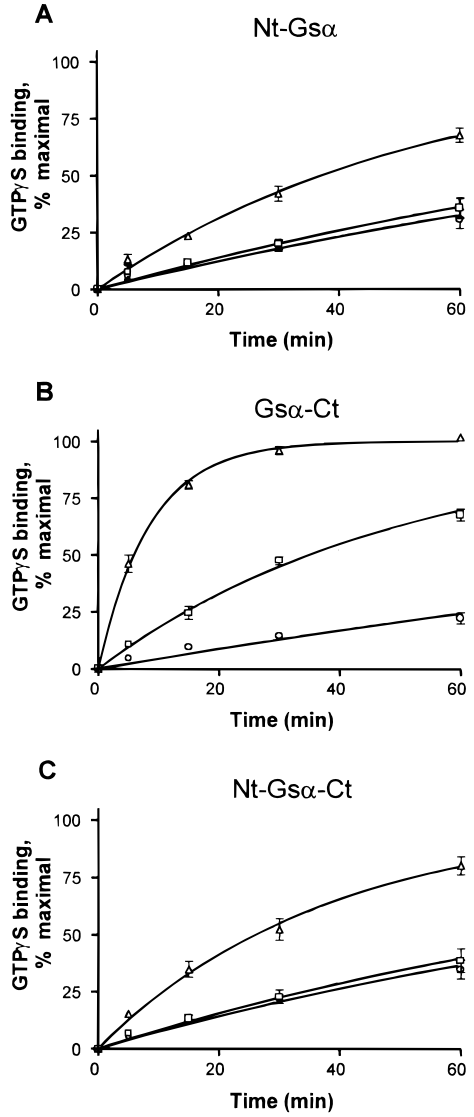

FIGURE 3: Time courses of GTPγS binding to Nt-Gsα, Gsα-Ct, and Nt-Gsα-Ct. The binding of GTPγS to Nt-Gsα (A), Gsα-Ct (B), or Nt-Gsα-Ct (C) (1 μM each) alone (□) or mixed with 2 μM Gtβγ (○) or 2 μM Gtβγ and uROS membranes (300 nM rhodopsin) (△) was initiated by addition of 5 μM [^{35}S]GTPγS. Gα-bound GTPγS was counted by withdrawing aliquots at the indicated times and passing them through Whatman cellulose nitrate filters (0.45 μm). GTPγS binding is expressed as percent of maximal, calculated based on protein concentration. The calculated k_{app} values (min^{-1}) are as follows: (A) 0.0075 ± 0.0005 (□), 0.0065 ± 0.0005 (○), 0.018 ± 0.001 (△); (B) 0.020 ± 0.001 (□), 0.0045 ± 0.0005 (○), 0.12 ± 0.01 (△); (C) 0.0085 ± 0.001 (□), 0.0075 ± 0.0005 (○), 0.027 ± 0.002 (△).

a more modest effect (k_{app} = 0.003 min^{-1}) (Figure 4). The basal GTPγS binding rates of all three Gtiα mutants were slightly increased in the presence of Gtβγ and potently stimulated with the joint addition of Gtβγ and R* (Figure 4).

GTPγS Binding Properties of His41Val Mutants of Ns-Gtiα and Gsα. If the increase of intrinsic GTPγS binding rate in Ns-Gtiα is caused by the His41 residue, the His41Val mutation in Ns-Gtiα would be expected to reverse this effect. Indeed, the Ns-GtiαHis41Val mutant displayed a large reduction in the intrinsic GTPγS binding rate (k_{app} = 0.0011 min^{-1}) relative to Ns-Gtiα (Figure 4, Table 1). The R*-stimulated GTPγS binding rate for Ns-GtiαHis41Val was similar to that for Ns-Gtiα (Figure 4). In the crystal structure

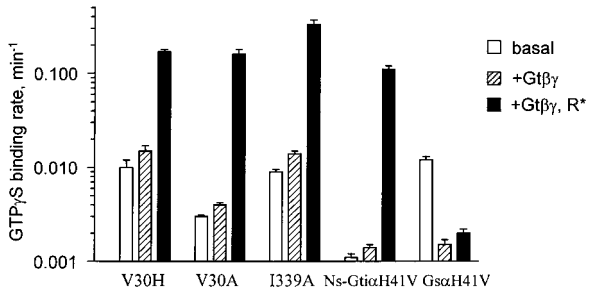

FIGURE 4: GTPγS binding rates of Gtiα and Gsα mutants. The binding of GTPγS to the Gtiα mutants Val30His, Val30Ala, and Ile339Ala and to the His41Val mutants of Ns-Gtiα and Gsα was measured, and the k_{app} values were calculated as described under Experimental Procedures.

of Gsα, the corresponding Gtα Val30 and Ile339 pair of residues, His41 and Ile383, also contact each other (*26*). To probe the role of this contact in Gsα, we substituted His41 by Val. The GsαHis41Val mutant showed only a relatively small decrease in the basal GTPγS binding rate ($k_{app} = 0.012$ min^{-1}) against Gsα ($k_{app} = 0.028$ min^{-1}), which can be further suppressed by addition of Gt$\beta\gamma$ ($k_{app} = 0.0015$ min^{-1}) (Figure 4, Table 1).

DISCUSSION

In vertebrate rod photoreceptors, the visual G-protein transducin couples light activation of rhodopsin to stimulation of cGMP phoshodiesterase (*1, 2*). Unlike Giα or Gsα, Gtα has a distinctively slow basal (unstimulated) rate of GDP/GTP exchange, which is essential for low noise signaling in photoreceptors. Another key attribute of Gt is its ability of very rapid activation by R*. During the time of photoresponse (~200 ms), a single molecule of R* may activate up to several hundred molecules of Gt (*1*), ensuring high signal amplification and, thus, high sensitivity of photoreceptors. What molecular features of Gtα provide for its high affinity to GDP in the absence of R*? The guanine nucleotide is bound in a deep cleft between the helical and p21ras-like domains of Gtα (*3*). Although the helical domain contributes very little to direct binding of GDP, it occludes guanine nucleotide from solvent and serves as a lid that prevents exit of GDP or GTP. The interdomain interactions, Asp146−Lys266 and Arg174−Glu39, which are preserved in both GDP- and GTP-bound conformations of Gtα (*3, 4*), may help to secure the nucleotide in the cleft. Similar interdomain contacts are present in Giα_1·GTPγS, but are lost in the GDP-bound conformation of Giα_1 (*27, 28*). This may in part account for the relatively low affinity of Giα for the nucleotide (*28*). The p21ras-like domain is a major contributor to the nucleotide binding energy. Five conserved motifs (G1−G5) from the p21ras-like domain and the linker 2 region participate in nucleotide binding (*3, 29*). Two of these motifs, G2 and G3, are localized within the conformation-sensitive switch regions I and II, respectively. The greater flexibility of the GDP binding regions and the low affinity of the GDP-bound Gsα, Giα, and Goα for Mg^{2+} may explain their high intrinsic GDP dissociation rates (*29*). It is likely that G$\beta\gamma$ inhibits the rate of GDP release by interacting with and stabilizing the Gα switch I and II regions. In contrast, the GDP binding regions in Gtα, primarily the switch regions, are probably more stable, leading to high affinity for GDP. Therefore, the already slow GDP dissociation rate of Gtα is seemingly unaffected by addition of Gt$\beta\gamma$. Apparently, the activational role of R* is to destabilize the GDP binding sites on Gtα, particularly the G5 site (the β6-α5 loop) through binding to the Gtα C-terminus/α4-β6 loop, and the G2/G3 regions via R*/Gt$\beta\gamma$ interaction. In addition to the C-terminus (Gtα-340−350) and the α4-β6 loop, the N-terminal region of Gtα is thought to be involved in an interaction with R* (*11*). Likewise, the N-termini of Goα and Gqα are believed to be important for Gα/receptor coupling (*13, 30*). This study supports a rather modest role of the 31 N-terminal residues of Gtα in the specific recognition of R*. Ns-Gtiα containing the Gsα N-terminus showed a lower rate of R*-induced GTPγS binding in comparison to Gtiα. If interaction between the N-terminus of Gtα and R* is comprised of several weak contacts, our results would be consistent with the mutational analysis of Gtα, which identified no N-terminal mutants outside the Gt$\beta\gamma$ contact residues with significantly impaired R* stimulation (*15*). To further the conclusion that the Gtα N-terminal sequence participates in the interaction with R*, we have generated and tested chimeric Gsα protein containing the Gtα N-terminal region, Nt-Gsα. Nt-Gsα was capable of weak stimulation by R*. Unfortunately, this chimera apparently had impairment of Gt$\beta\gamma$ binding, precluding more accurate examination of the interaction with R*. Nonetheless, the role of the N-terminal sequence of Gtα in interaction with R* might be more essential than it is implied by our results. All tested chimeric proteins had the His6-tag at the N-terminus instead of native myristoyl modification. The lipid insertion into the membrane might be required to fully engage the N-terminal sequence of Gtα in an interaction with R*.

Results of this study highlight a different role of the Gtα N-terminus—its involvement in regulation of the low rate of Gtα intrinsic GDP/GTP exchange. We found that replacement of the Gtα N-terminus in Gtiα by the N-terminal domain from Gsα resulted in a substantial increase in the basal GTPγS binding rate. Furthermore, a single amino acid residue at the position corresponding to GtαVal30 (His41 in Gsα) appears to be primarily responsible for the observed effect. Mutants of Gtiα with single substitutions of Val30 by His and Ala exhibited ~8- and 2-fold increases in the basal GTPγS binding rate, respectively. The basal rates of Ns-Gtiα and the GtiαVal30 mutants were not inhibited by Gt$\beta\gamma$. The crystal structures of Gtα show the Val residue interacting with the C-terminal Ile339 at the C-terminal end of the α5 helix (*3, 4*). The GtiαIle339Ala mutant also displayed a significantly higher basal GTPγS binding rate. Thus, the interaction between Val30 and Ile339 is likely to stabilize the overall GDP-bound conformation of Gtα, and especially the α5 helix and the guanine binding β6-α5 loop. Destabilization of the β6-α5 loop in the Val30 and Ile339 mutants is consistent with the lack of the Gt$\beta\gamma$ inhibitory effect on the enhanced intrinsic GTPγS binding rates since binding of Gt$\beta\gamma$ is not expected to directly affect this region of Gtα. A similar mechanism involving stabilization of the α5 helix through interactions with the N-terminal domain has been proposed to explain decreased apparent affinities for GDP seen in C-terminally truncated Goα and Giα (*16, 17*). Truncation of residues corresponding to Gtα ^{338}Ile-Ile-Ile^{340} was necessary to yield the low-GDP-affinity phenotype (*17*). In Gsα, His41 also makes a van der Waals contact with the C-terminal Ile residue (*26*). This contact appears to

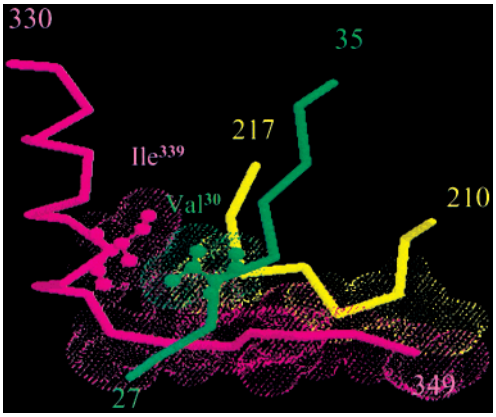

FIGURE 5: A two-site interaction of the Gtα C-terminus with the α2-β4 loop and the N-terminal region. A view of the N-terminal region, Gtα-27−35 (green), the α2-β4 loop (yellow), and the C-terminus (magenta) based on the structure of GtαGTPγS (*3*). The contact residues, Val30 and Ile339, are shown in "ball-and-stick" representation. The α2-β4/C-terminus linkage is formed by van der Waals contacts between residues 212, 213, and 215 from the α2-β4 loop and C-terminal residues 343−349. The image was generated using RasMol (v.2.6).

be weaker than the hydrophobic interaction between Val and Ile, possibly explaining a relatively small increase in affinity for GDP caused by the His41Val mutation of Gsα. Interestingly, replacement of the 42 N-terminal residues of Gsα by the Gtα residues led to a more significant increase in GDP affinity.

We speculate that in addition to the Val-Ile contact, which is present in all three Gα subunits (Gtα, Giα, and Goα), a second interaction between more distal C-terminal residues, Gtα-343−349, and the switch II residues, Gtα-212−215, helps to maintain the lower basal Gtα GDP/GTP exchange rate. The latter interaction was first identified in one of the GtαGTPγS crystal structures (*3*). Recently, we have shown that this interaction is likely present in the GDP-bound Gtα as well (*23*). Such an interaction would be weak, if possible at all, in Goα as it contains the Asp residue at the position occupied by Gtα Gly213. The Asp side chain at this position would cause multiple steric hindrances with the C-terminal residues, thus disrupting a potential interaction (*23*). The lack of stable interactions between switch II and the C-terminus in Goα is supported by a notably smaller effect of the C-terminal 10 residue deletion vs the 14 residue deletion on Goα affinity for GDP (*16*).

A view of the interacting sites, Val30 with adjacent residues, the α2-β4 loop, and the C-terminus, is shown in Figure 5. The coordinates of the Gtα·GTPγS structure were used as the C-terminal residues are not resolved in the Gtα·GDP structure. However, positions of Val30 and the contact residues, Glu212, Gly213, and Thr215, from the α2-β4 loop are almost identical in Gtα·GTPγS and Gtα·GDP (*3*, *4*). The two-site interaction of the Gtα C-terminus with switch II and the N-terminal Val30 perhaps explains a larger GDP affinity decrease in the GtiαVal30His mutant relative to the GtiαVal30Ala mutant. The Val30Ala mutant may have weakened or lost contact with Ile339, whereas the larger His side chain may also disrupt the switch II/C-terminus contacts by pushing the C-terminus away from the interaction site. Overall, our data suggest that the stabilizing interaction between the N- and C-terminal regions of Gtα together with the switch II/C-terminus coupling play important roles in maintaining a uniquely low rate of Gtα intrinsic GDP/GTP exchange.

REFERENCES

1. Chabre, M., and Deterre, P. (1989) *Eur. J. Biochem. 179*, 255−266.
2. Yarfitz, S., and Hurley, J. B. (1994) *J. Biol. Chem. 269*, 14329−14332.
3. Noel, J. P., Hamm, H. E., and Sigler, P. B. (1993) *Nature 366*, 654−663.
4. Lambright, D. G., Noel, J. P., Hamm, H. E., and Sigler, P. B. (1994) *Nature 369*, 621−628.
5. Lambright, D. G., Sondek, J., Bohm, A., Skiba, N. P., Hamm, H. E., and Sigler, P. B. (1996) *Nature 379*, 311−319.
6. Iiri, T., Farfel, Z., and Bourne, H. R. (1998) *Nature 394*, 35−38.
7. West, R. E., Jr., Moss, J., Vaughan, M., Liu, T., and Liu, T. Y. (1985) *J. Biol. Chem. 260*, 14428−14430.
8. van Dop, C., Yamanaka, G., Steinberg, F., Sekura, R. D., Manclark, C. R., Stryer, L., and Bourne, H. R. (1984) *J. Biol. Chem. 259*, 23−26.
9. Garcia, P. D., Onrust, R., Bell, S. M., Sakmar, T. P., and Bourne, H. R. (1995) *EMBO J. 14*, 4460−4469.
10. Osawa, S., and Weiss, E. R. (1995) *J. Biol. Chem. 270*, 31052−31058.
11. Hamm, H. E., Deretic, D., Arendt, A., Hargrave, P. A., Koenig, B., and Hofmann, K. P. (1988) *Science 241*, 832−835.
12. Phillips, W. J., Wong, S. C., and Cerione, R. A. (1992) *J. Biol. Chem. 267*, 17040−17046.
13. Taylor, J. M., Jacob-Mosier, G. G., Lawton, R. G., Remmers, A. E., and Neubig, R. R. (1994) *J. Biol. Chem. 269*, 27618−27624.
14. Bigay, J., Faurobert, E., Franco, M., and Chabre, M. (1994) *Biochemistry 33*, 14081−14090.
15. Onrust, R., Herzmark, P., Chi, P., Garcia, P. D., Lichtarge, O., Kingsley, C., and Bourne, H. R. (1997) *Science 275*, 381−384.
16. Denker, B. M., Schmidt, C. J., and Neer, E. J. (1992) *J. Biol. Chem. 267*, 9998−10002.
17. Denker, B. M., Boutin, P. M., and Neer, E. J. (1995) *Biochemistry 34*, 5544−5553.
18. Papermaster, D. S., and Dreyer, W. J. (1974) *Biochemistry 13*, 2438−2444.
19. Yamanaka, G., Eckstein, F., and Stryer, L. (1985) *Biochemistry 24*, 8094−8101.
20. Kleuss, C., Pallat, M., Brendel, S., Rosenthal, W., and Scultz, G. (1987) *J. Chromatogr. 407*, 281−289.
21. Natochin, M., and Artemyev, N. O. (1998) *Biochemistry 37*, 13776−13780.
22. Skiba, N. P., Bae, H., and Hamm, H. E. (1996) *J. Biol. Chem. 271*, 413−424.
23. Natochin, M., Muradov, K. G., McEntaffer, R. L., and Artemyev, N. O. (2000) *J. Biol. Chem. 275*, 2669−2675.
24. Natochin, M., and Artemyev, N. O. (1998) *J. Biol. Chem. 273*, 4300−4303.
25. Higashijima, T., Ferguson, K. M., Sternweis, P. C, Smigel, M. D., and Gilman, A. G. (1987) *J. Biol. Chem. 262*, 762−766.
26. Sunahara, R. K., Tesmer, J. J. G., Gilman, A. G., and Sprang, S. R. (1997) *Science 278*, 1943−1947.
27. Coleman, D. E., Berghuis, A. M., Lee, E., Linder, M. E., Gilman, A. G., and Sprang, S. R. (1994) *Science 265*, 1405−1412.
28. Mixon, M. B, Lee, E., Coleman, D. E., Berghuis, A. M., and Gilman, A. G., and Sprang, S. R. (1995) *Science 270*, 954−960.
29. Sprang, S. R. (1997) *Annu. Rev. Biochem. 66*, 639−678.
30. Kostenis, E., Zeng, F. Y., and Wess, J. (1998) *J. Biol. Chem. 273*, 17886−17892.

BI992156L